A Surface-Potential-Based Compact Model for AlGaN/GaN MODFETs

Xiaoxu Cheng and Yan Wang

***Abstract*—In this paper, a surface-potential-based (SP-based) model for AlGaN/GaN modulation-doped field-effect transistors (MODFETs) is built for the first time. First, a closed-form analytical approximation for the Fermi potential E_F relative to the bottom of the conduction band at the AlGaN/GaN interface is presented and verified to be accurate enough under different biases and temperatures. Then, the potential of the bottom of the conduction band at the AlGaN/GaN interface φ_s is defined as the SP, and the value of φ_s relative to ground is calculated. The development of SP-based compact dc model is achieved based on this calculation. Velocity saturation, channel length modulation, drain-induced barrier lower effect, and self-heating effect are included in the presented model. Compared with the $V_{\rm th}$-based model developed by our group, this SP-based model provides a symmetric and more accurate but simpler description for AlGaN/GaN MODFETs. The calculated dc characteristics and transconductance for devices with different lengths are in excellent agreement with the experimental data over the full range of applied gate and drain biases and under different temperatures.**

***Index Terms*—AlGaN/GaN modulation-doped field-effect transistors (MODFETs), compact model, surface potential (SP).**

I. Introduction

COMPARED with surface-potential-based (SP-based) models, the threshold-voltage-based ($V_{\rm th}$-based) models have encountered severe limitations [1], [2] since they are usually developed using regional approximations that are joined together by suitable smoothing functions over the moderate inversion region [1], [3], [4]. With the power supply voltage scaled toward the 1.2-V level, the moderate inversion region becomes a significant fraction of the voltage swing, essentially invalidating a $V_{\rm th}$-based model [5]. Thus, the SP-based models for MOSFETs have been emphasized as the next generation compact MOSFETs models [6].

When applied to AlGaN/GaN modulation-doped field-effect transistors (MODFETs), the problems of $V_{\rm th}$-based models worsen. As we know, the definition of $V_{\rm th}$ is usually based on the E_F (take the bottom of conduction as a reference) at the source end under an assumption that this E_F keeps unchanged along the channel [7], [8]. This assumption is acceptable at least for MOSFETs working in strong inversion region because the carrier concentration n_s will exponentially increase with E_F, and this increasing n_s helps in pinning E_F. However, energy quantization in AlGaN/GaN heterojunctions caused by strong quantum confinement weakens the n_s dependence on E_F; it is physically expected that E_F can no longer be pinned and will vary a lot under different gate-to-channel voltages. This variation is also confirmed by numerical and analytic results that will be shown later in this paper. Neglecting this variation to define $V_{\rm th}$ will obviously bring some inherent errors into the model. Moreover, the asymmetry introduced by a source-referenced threshold voltage can also cause the singular behavior of d^2I_{ds}/dV_{ds}^2 at $V_{ds}=0$ and make the model problematical in IM3 simulation [9], which is very important for a radio-frequency circuit design. The solution of the aforementioned problems stimulates the development of the SP-based model for AlGaN/GaN MODFETs because this model can afford the clear and accurate physical content and has the ability to provide a single expression for all the regions of operation and the inherently symmetric nature.

What impedes the progress of the SP-based models is the need for elaborate computations of φ_s for MOSFETs or E_F for AlGaN/GaN MODFETs, which is usually given by an implicit transcendental function. This problem has been excellently solved for MOSFETs by using an approximate analytical solution [10], but it is quite different for AlGaN/GaN MODFETs because of the strong quantum mechanical effects. To the best of our knowledge, there was no attempt on analytically solving this problem being reported before. A similar work to calculate φ_s is the development of a fitting expression for $E_F \sim n_s$ (n_s is the density of the 2DEG) relationship given by Kola *et al.* [11]. In this expression, three device-size and temperature-dependent parameters are used, and the accuracy of this expression is about 0.01 V, which does not meet the requirement of the SP-based models to accurately reproduce the derivatives of the current. Thus, one purpose of this paper is to introduce a closed-form analytical approximation for E_F that is computationally efficient, well behaved, and accurate enough for various devices under different bias and temperature conditions. Using this analytical approximation, ground referenced φ_s for AlGaN/GaN MODFETs is defined, and this concept enables the development of SP-based compact model for AlGaN/GaN MODFETs.

This paper is arranged as follows. The basic physics for this model is first discussed, and an explicit method to calculate E_F and the definition of φ_s are given. In Section II, the mobility model for AlGaN/GaN MODFETs is rewritten, and the I–V characteristics of the model based on φ_s is developed in Section II. Drain-induced barrier lower (DIBL) and self-heating effects are also included in this model, and the modeling results are compared with several experimental measurements in Section III. This paper is concluded in Section IV.

Manuscript received June 27, 2010; revised August 21, 2010 and October 7, 2010; accepted October 19, 2010. Date of publication December 6, 2010; date of current version January 21, 2011. This work was subsidized by Special Funds for Major State Basic Research Projects 2010CB327504. The review of this paper was arranged by Editor S. Bandyopadhyay.

The authors are with the Institute of Microelectronics, Tsinghua University, Beijing 100084, China (e-mail: wangy46@tsinghua.edu.cn).

Digital Object Identifier 10.1109/TED.2010.2089690

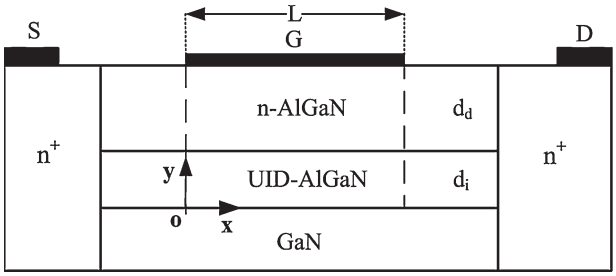

Fig. 1. Cross-sectional view of a general AlGaN/GaN MODFET with gate length L, n-AlGaN layer thickness d_d, and space layer thickness d_i.

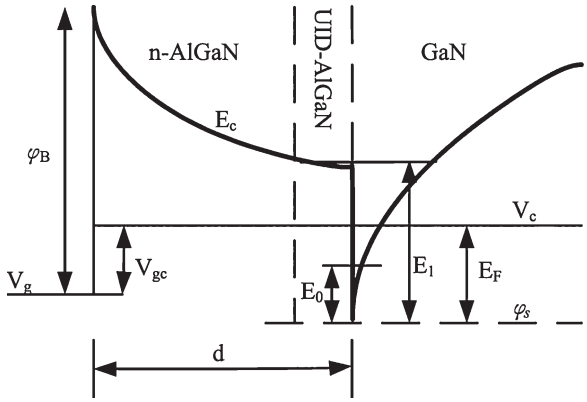

Fig. 2. Energy band diagram of AlGaN/GaN MODFETs for nonzero gate bias. φ_B is the barrier height of the gate Schottky junction. E_F is the Fermi potential relative to the bottom of the conduction band. E_0 and E_1 are the potential of the two allowed energy band in the triangular well. φ_s is the surface potential. V_g is the gate potential, and V_c denotes the channel potential. φ_s, V_g, and V_c are all ground referenced.

II. Model Description

The cross-sectional view of an AlGaN/GaN MODFET discussed in this paper is shown in Fig. 1. The under-gate-energy-band diagram for positive gate bias is shown in Fig. 2. High-density 2DEG forms at the heterointerface due to the discontinuity of the conduction band and polarization-induced charge at the heterointerface.

A. Computation of E_F and Definition of the SP

One of the key problems in the compact model development is that the relative Fermi level E_F is an implicit function of the gate potential V_g and the channel potential V_c. The sheet carrier density n_s and the offset voltage $V_{\rm off}$ of the AlGaN/GaN MODFETs are given by the following [8], [12]:

$$n_s = \frac{\varepsilon}{\rm qd}(V_g - V_{\rm off} - V_c - E_F) \tag{1}$$

$$V_{\rm off} = \varphi_B - \Delta E_C - \frac{\rm qN_D d_d^2}{2\varepsilon} - \frac{q\sigma}{\varepsilon}(d_d + d_i) \tag{2}$$

$$n_s = {\rm DkT}\ln\left(1 + \exp\left(\frac{(E_F - E_0)}{v_q}\right)\right) \tag{3}$$

$$E_0 = u_1 n_s^{2/3}. \tag{4}$$

The definitions of related symbols are given in Table I. Equations (1) and (2) can be obtained from the solution of Poisson equations under the assumption that the ionization in n-AlGaN layer is complete, and the unintentionally doped AlGaN layer is neutral. Equation (3) is obtained from the solution of the Schrodinger's equations on the basis of an approximate triangular potential distribution. In the calculation, only the lowest allowed energy band E_0 is considered because $E_1 \approx 3E_0$, and the electron contributed by E_1 and higher energy band can be neglected.

TABLE I
List of Symbols

Symbols	Physics meaning
n_s	the density of the 2DEG
q	the electron charge
ε	the permittivity of AlGaN
D	the total thickness of the AlGaN layer
$\varphi_{\rm B}$	the barrier height of the gate schottky junction
N_D	the doping concentration of the n-AlGaN
σ	the polarization induced charge density at the heterointerface
D	the conduction band density of states of a 2D system
k	the Boltazmann's constant.
T	the ambient temperature
v_q	thermal voltage, v_q=kT/q
u_1	position of E_0 determined by Robin boundary condition [9]

The search for an approximate analytical solution begins with an asymptotic solution of (1)–(4) under different mathematical conditions of (1)–(4). This asymptotic solution is refined to obtain a final solution with accuracy of about picovolt. To simplify the description and the coding of this approximate solution, we use the following denotation: $c_{\rm ox} = q\varepsilon/d$, $a = {\rm DkT}$, $a_1 = a/c_{\rm ox}$, and $v_{\rm go} = V_g - V_{\rm off} - V_c$. The procedure of our algorithm is then divided into the following two steps:

1) The calculation of an asymptotic solution: η

We also take a reference voltage $v_{\rm gr}$ to denote the value of $v_{\rm go}$ when $E_F = E_0$. It can be explicitly obtained from (1)–(4), i.e.,

$$v_{\rm gr} = a_1\ln(2) + u_1 a^{2/3}\ln(2)^{2/3}. \tag{5}$$

For $v_{\rm go} \geq v_{\rm gr}$, noticing that $exp((E_F - E_0)/v_q) \gg 1$, we give η as follows:

$$\eta = \frac{u_1(c_{\rm ox}v_{\rm go})^{2/3} + \left(v_{\rm go} - v_{\rm gr}^2/(v_{\rm go} + v_q)\right)v_q/a_1}{1 + v_q/a_1 + 2u_1(c_{\rm ox}v_{\rm go})^{2/3}/3v_{\rm go}}. \tag{6}$$

For $v_{\rm go} < v_{\rm gr}$, noticing that the value of $ln(1 + \exp((E_F - E_0)/v_q))$ slowly varies with $v_{\rm go}$, we can use a second-order polynomial expression to estimate it. Two reference voltages $v_{\rm gr1}$ and $v_{\rm gr2}$ are used to denote the value of $v_{\rm go}$ when $E_F - E_0 = -3v_q$ and $-2v_q$, respectively. While both reference voltages can be obtained explicitly, η is calculated as follows:

$$x_1 = v_{\rm gr} - v_{\rm gr1} \tag{7}$$

$$x_2 = v_{\rm gr} - v_{\rm gr2} \tag{8}$$

$${\rm bb} = \left(0.6445x_2^2 - 0.2647x_1^2\right)/x_1x_2(x_2 - x_1) \tag{9}$$

$${\rm aa} = (0.6445x_1 - 0.2647x_2)/x_1x_2(x_2 - x_1) \tag{10}$$

$$s_0 = {\rm aa}(v_{\rm go} - v_{\rm gr1})^2 + {\rm bb}(v_{\rm go} - v_{\rm gr1}) + \ln(1 + e^{-3}) \tag{11}$$

$$\eta = v_{\rm go} - a_1 s_0. \tag{12}$$

2) The refinement of the asymptotic solution to obtain a better approximate solution: E_F

While η is a crude initial approximation to E_F, it is not accurate enough. To obtain a more accurate solution, a small refinement w is introduced, and E_F is calculated as

$$E_F = \eta + w. \tag{13}$$

Combining (1), (3), and (13), we can obtain the following:

$$1 + \exp\left(\frac{(\eta + w) - u_1\left(c_{\rm ox}\left(v_{\rm go} - (\eta + w)\right)\right)^{\frac{2}{3}}}{v_q}\right) = \exp\left(\frac{(v_{\rm go} - (\eta + w))}{a_1}\right). \tag{14}$$

The second-order Taylor expansion of (14) yields to the following equations to determine w:

$$\eta_1 = u_1\left(c_{\rm ox}(v_{\rm go} - \eta)\right)^{2/3} \tag{15}$$
$$e_1 = \exp\left((\eta - \eta_1)/v_q\right) \tag{16}$$
$$e_2 = \exp\left((v_{\rm go} - \eta)/a_1\right) \tag{17}$$
$$c_0 = (1 + e_1 - e_2)/e_2 \tag{18}$$
$$s_1 = -2\eta_1/3(v_{\rm go} - \eta) \tag{19}$$
$$c_1 = (1 - s_1)e_1/e_2 + v_q/a_1 \tag{20}$$
$$c_2 = \left(\frac{\eta_1 v_b}{9(v_{\rm go} - \eta)^2} + 0.5(1 - s_1)^2\right)e_1/e_2 - 0.5v_q^2/a_1^2 \tag{21}$$
$$w = -2v_q c_0/\left(c_1 + \sqrt{c_1^2 - 4c_2 c_0}\right). \tag{22}$$

Equations (15)–(22) are calculated twice to further refine the result of E_F, and the obtained accuracy is about 15 pV, which is enough for further current and charges derivatives. Using this result, we can define the SP φ_s as the bottom of the conduction band, and it is easy to find $\varphi_s = E_F + V_c$. V_c is equal to V_s at the source end of the channel and to V_d at the drain end of the channel. We can find that in the Si MOSFETs, the SP indicates the Si/SiO_2 interface potential, whereas in GaN MODFETs, the SP and the AlGaN/GaN interface potential have the same meaning. Based on this definition, the SP at the source and the drain sides can be separately calculated. We denote these two potentials as φ_{ss} and φ_{sd}, and an SP-based compact model for AlGaN/GaN MODFETs can be developed.

B. Mobility Model

In the low-field region where the longitudinal electric field along the channel E_x is less than the critical field E_T, the electron drift velocity can be calculated as [4]

$$v(E_x) = \frac{\mu_{\rm LF} E_x}{1 + u_a E_x/E_T} \tag{23}$$

where $\mu_{\rm LF}$ is low longitudinal field mobility. Physically, the 2DEG mobility is dependent on its density [13], which is related to the vertical field in the GaN layer. In this paper, a mobility model is introduced based on the phenomenological model we used in our previous model [4], i.e.,

$$\mu_{\rm LF} = \frac{\mu_0}{1 + p_1 E_{y,\rm eff} + p_2 E_{y,\rm eff}^2} \tag{24}$$

where μ_0 is the low field mobility, p_1 and p_2 are both the fitting parameters, which can be extracted from the experimental data, and $E_{y,\rm eff}$ denotes the effective vertical field in the GaN layer. The SP midpoint is used in $E_{y,\rm eff}$ calculation to conserve the model symmetry, and (25) can be obtained by the following:

$$E_{y,\rm eff} = \frac{\varepsilon\left(V_{\rm go} - (\varphi_{ss} + \varphi_{sd})/2\right)}{d\varepsilon_{\rm GaN}} = \frac{\varepsilon(V_{\rm go} - \varphi_{\rm sm})}{d\varepsilon_{\rm GaN}}. \tag{25}$$

C. I–V Characteristics Model

Based on the definition of the SP, the channel charge density can simply be calculate as

$$n_s = c_{\rm ox}(V_{\rm go} - V_{\rm off} - \varphi_s). \tag{26}$$

Under the assumption of the gradual channel approximation and the drift-diffusion model [14], the current density j_n can be written as

$$j_n = q u_n n_s \frac{\partial \varphi_s}{\partial x} {\rm q D}_n \frac{\partial n_s}{\partial x}. \tag{27}$$

Using Einstein relation ($D_n = \mu_n V_q$) and combining with (23), the drain current I_{ds} can be written as

$$I_{ds} = W q c_{\rm ox} \frac{\mu_{\rm LF}}{1 + \mu_a \frac{\partial \varphi_s/\partial x}{E_C}}(V_{gs} - V_{\rm off} - \varphi_s + v_q)\frac{\partial \varphi_s}{\partial x}. \tag{28}$$

Integrating (28) from the source side to the drain side, the current can be calculated as follows:

$$I_{ds} = \beta \mu_{\rm LF} \frac{(V_{gs} - V_{\rm off} + v_q - \varphi_{\rm sm})\varphi}{1 + \delta_0 \varphi \mu_a / V_{\rm CL}} \tag{29}$$

where $\beta = {\rm qc_{ox}} W/L$, $V_{\rm CL} = E_T L$, and $\varphi = \varphi_{sd} - \varphi_{ss}$. The terminal voltage dependence enters through φ_{ss} and φ_{sd}, which are implicit functions of the bias. Although the SP-based model is inherently symmetry, there are other problems that come from the singular nature of the velocity saturation model (23) [15]. To avoid this problem, a variable δ_0 is introduced to assure $(d^2 I_{ds}/dV_{ds}^2)_{V_{ds}=0} = 0$, which is an important manifestation of the model symmetry. Like in other SP-based models, $\delta_0 = \varphi/(\varphi + gV_{\rm CL})$, where g is a small constant [5].

In our model, the saturation voltage $V_{\rm dsat}$ is defined as the drain bias when the longitudinal electric field reaches the critical field E_T. The channel potential in the velocity-saturation regions can thus be expressed as [8]

$$V_{ds} = V_{\rm dse} + {\rm pE}_T \sinh(\Delta L/p) \tag{30}$$

where $V_{\rm dse}$ is the potential at the end of the gradual channel region, and ΔL is the length of the velocity-saturation region. To avoid solving the equation set, a smooth transition from the

linear to saturation regions can be modeled by the following smoothing function:

$$V_{\rm dse} = \frac{V_{ds}}{(1 + (V_{ds}/V_{\rm dsat})^m)^{1/m}} \tag{31}$$

where m is a positive factor. ΔL can now be evaluated by (30), and the drain current I_{ds} including this channel length modulation effect can be finally written as

$$I_{ds} = \beta\mu_{\rm LF}\frac{(V_{gs} - V_{\rm off} + V_q - \varphi_{\rm sm})\varphi}{r_L + \delta_0\varphi\mu_a/V_{\rm CL}} \tag{32}$$

where $r_L = (1 + \Delta L/L)^{-1}$. This formula is now similar to a typical SP model [5], and the model symmetry is well conserved.

D. Self-Heating and DIBL Effect

As higher power and shorter channel AlGaN/GaN MODFETs are fabricated, self-heating and DIBL effects have to be taken into account in a compact model. Because the analytical solution for φ_s developed here has already included the temperature term, there is no need to introduce several parameters to describe the temperature effect on φ_s, as we have used in [16]. The other features of this calculation method are directly implanted in this model.

The deduction of (1) is based on the gradual-channel approximation that neglects the lateral field gradient in the Poisson equation [3]. When the device is scaling down and the channel length is shrinking, this lateral gradient cannot be neglected any longer. An efficient way to consider short-channel effect in AlGaN/GaN MODFETs model is by introducing a shift to the offset voltage $\Delta V_{\rm off}$. A 2-D Poisson equation in the AlGaN layer must be solved to obtain this voltage [17]. However, the boundary condition of this Poisson equation is not well defined, and the use of some adjustable model parameters actually leads to a semiempirical expression. In this paper, we simply assume $\Delta V_{\rm off} = V_{ds}/{\rm SCE1}$, and SCE1 is a parameter that is dependent on channel length L.

III. Results and Discussion

Comparison of this analytical solution with the result of numerical solution of (1)–(4) is shown in Figs. 3 and 4. Excellent accuracy is achieved over a wide range of bias condition and device parameter, and the absolute error introduced by our analytical approximation is under 15 pV. Noticing that this method requires computation of only four exponent and two square roots, the central processing unit time required to compute E_F is also acceptable in a compact model. It is confirmed in Figs. 3 and 4 that E_F varies a lot along with the applied gate bias because of the quantum confinement effect. This variation brings some inherent error into the $V_{\rm th}$-based model. It is also found that this model error is increased with the scaling down of AlGaN/GaN MODFETs because the E_F variation is more significant. Thus, it is necessary to use this SP-based model that can take this variation into account.

The symmetry and continuity of this SP-based model is illustrated in Fig. 5. It is easy to find that this model is symmetric

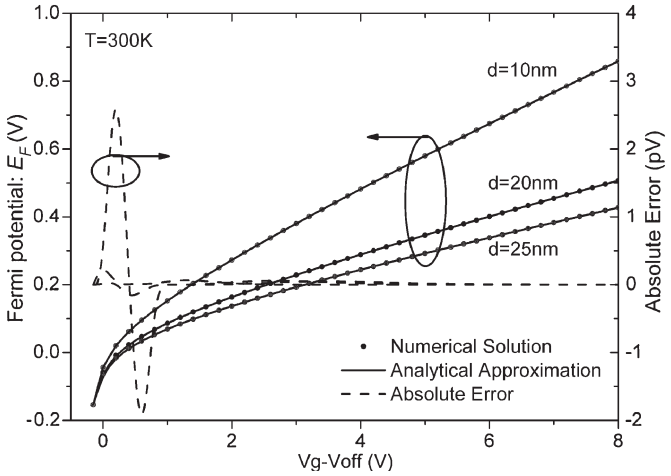

Fig. 3. Comparison of the analytical approximation of the E_F with numerical solution for AlGaN/GaN MODFETs under different AlGaN layer thickness; $T = 300$ K. $V_c = 0$.

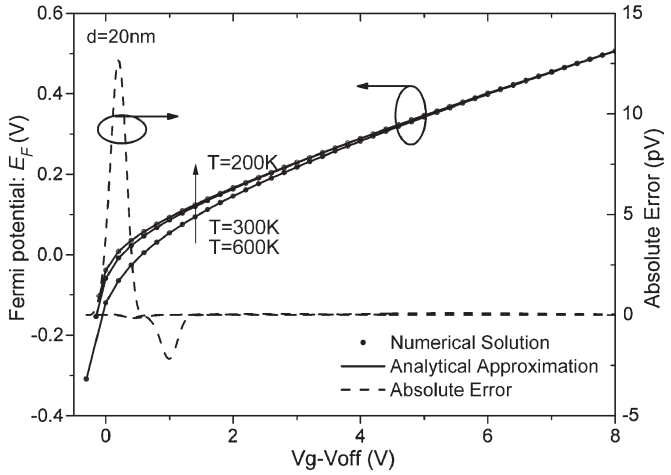

Fig. 4. Comparison of the analytical approximation of the E_F with numerical solution for AlGaN/GaN MODFET under different temperatures; the AlGaN layer thickness $d = 20$ nm. $V_c = 0$.

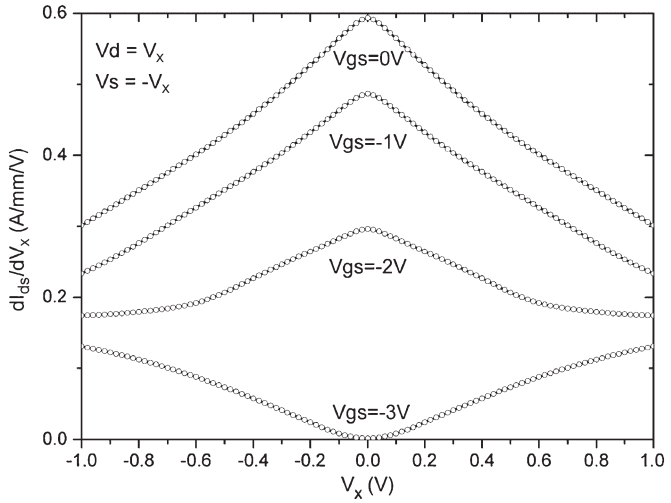

Fig. 5. Typical Gummel symmetry test for $Al_{0.5}Ga_{0.5}N$/GaN MODFET. $W = 1$ mm, $L = 1$ μm, $d = 20$ nm, $V_s = -V_x$, and $V_d = V_x$.

TABLE II
PARAMETERS USED IN THE CALCULATION FOR THE DIFFERENT DEVICES

parameter	Quantity	Fig.6 Fig.7	Fig.8 Fig.9	Fig.10
V_{off}(V)	the offset voltage	-2.9	-3.97	-3.0
Rs(Ω)	parasitic source resistance	0.13	0.45	1.1
Rd(Ω)	parasitic drain resistance	0.43	1.1	2
W(μm)	Gate width	75	25	250
L(μm)	gate length	1	0.7	0.35
d_i(nm)	spacer layer thickness	3	3	5
d_d(nm)	n-AlGaN layer thickness	22	15	25
E_T(10^5V/m)	critical electric field	178	150	178
u_a	parameter	3.64	2.1	3.22
pp[a]	parameter	1	2.1	1
μ_0(m^2/V/s)	parameter	0.08	0.03	0.06
p_1(m V^{-1})	parameter	1.13	-0.21	0.94
p_2(m^2 V^{-2})	parameter	0.125	0.117	0.44
$SCE1$	SCE parameter	600	680	30
Rth(K/W)	Thermal resistance	6	21	56

[a]In the model we use $p=pp\bullet 2d/\pi$, for calculation.

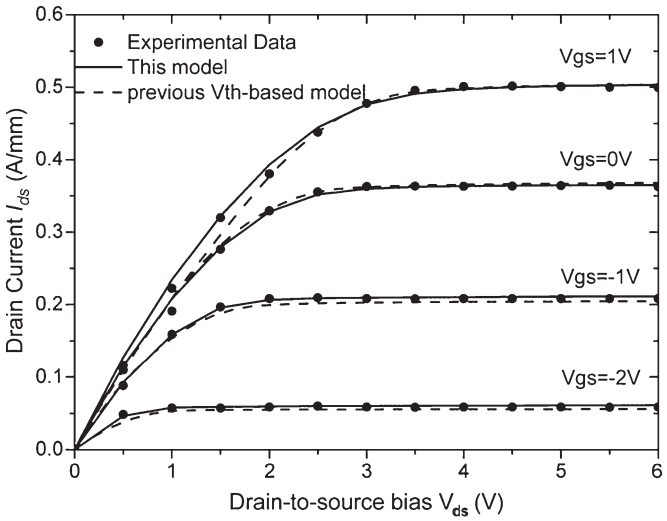

Fig. 6. Calculated and measured I–V characteristics for an $Al_{0.15}Ga_{0.85}N$/GaN MODFET. V_{gs} is swept from -2 to 1 V at a step of 1 V. (Solid line) The results of the presented SP-based model are compared with (dash line) the $V_{\rm th}$-based model and (symbol) the experimental data [18].

with respect to source–drain interchange (sometimes called Gummel symmetry) and has no d^2I_{ds}/dV_{ds}^2 singularity because this model for AlGaN/GaN MODFETs is inherently symmetric as other SP models for MOSFET. It is well known that the smooth behavior shown at $V_x = 0$ enables a compact mode to reproduce correct 3 dB/dB slope of the third harmonic [5].

To demonstrate the accuracy of this SP-based model, comparative experimental results from MODFETs devices of two different Al mole fractions are first chosen: $Al_{0.15}Ga_{0.85}N$/GaN [18] and $Al_{0.50}Ga_{0.50}N$/GaN [19]. The calculation results of this SP-based model are compared with our previous $V_{\rm th}$-based model developed in [1] and [4], and the parameters for these devices used in this model are shown in Table II.

The variation of the drain current I_{ds} with drain-to-source voltage V_{ds} for an $Al_{0.15}Ga_{0.85}N$/GaN is plotted along with the measurement results [18] and the $V_{\rm th}$-based model in Fig. 6. Although the equation set to describe the voltage balance between

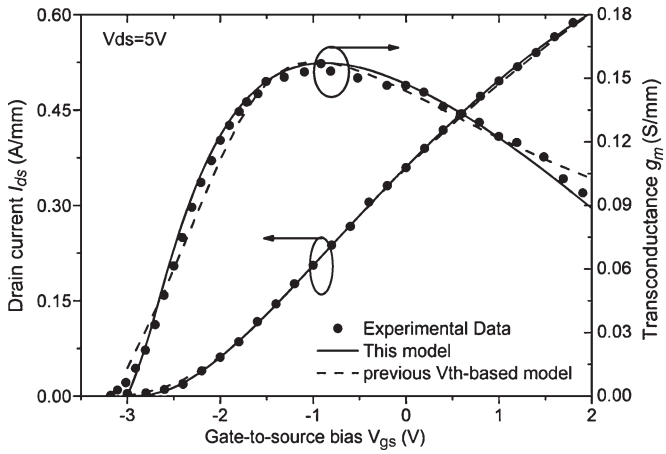

Fig. 7. Calculated and measured dc transfer characteristics for an $Al_{0.15}Ga_{0.85}N$/GaN MODFET. V_{gs} is swept from -3 to 2 V, and V_{ds} is 5 V.

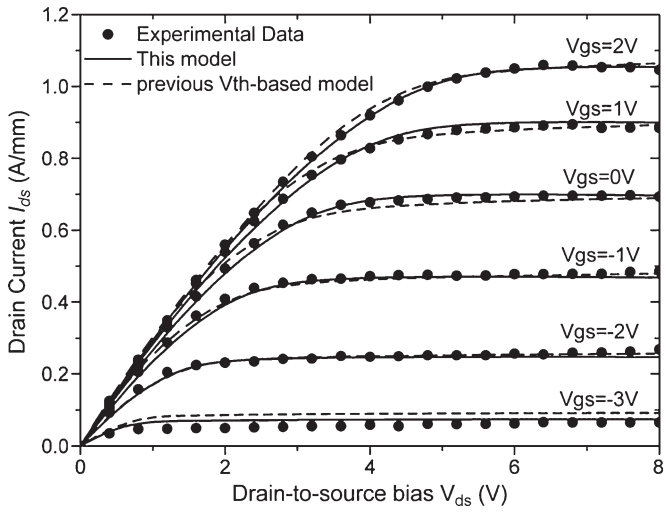

Fig. 8. Calculated and measured I–V characteristics for an $Al_{0.50}Ga_{0.50}N$/GaN MODFET. V_{gs} is swept from -3 to 2 V at a step of 1 V. (Solid line) The results of the presented SP-based model are compared with (dash line) the $V_{\rm th}$-based model and (symbol) the experimental data [19].

the gradual-channel region and the velocity-saturation region used in [1] is replaced by a much simpler formula, i.e., (30), this model provides a more accurate description than the previous $V_{\rm th}$-based model. Thus, the channel length modulation effect can be well described. The dc transfer characteristics along with the transconductance are shown in Fig. 7, and an excellent agreement between our calculation and the experimental data is obtained when the gate-to-source bias is above the offset voltage $V_{\rm off}$. When the applied gate-to-bias voltage is very low, little discrepancy of this model originates in the imprecise triangular potential approximation.

A further comparison to the experimental results is obtained by analyzing an $Al_{0.50}Ga_{0.50}N$/GaN MODFET. The calculated output characteristics along with the experimental results are shown in Fig. 8. We can find that the present SP-based model shows much closer results to the measurement data than the previous $V_{\rm th}$-based model in the linear region. This result can be expected because the SP-based model uses φ_s as a key variable in the model development, whereas the $V_{\rm th}$-based model collapses the complicated $\varphi_s(V_{\rm go})$ dependence shown in Figs. 3

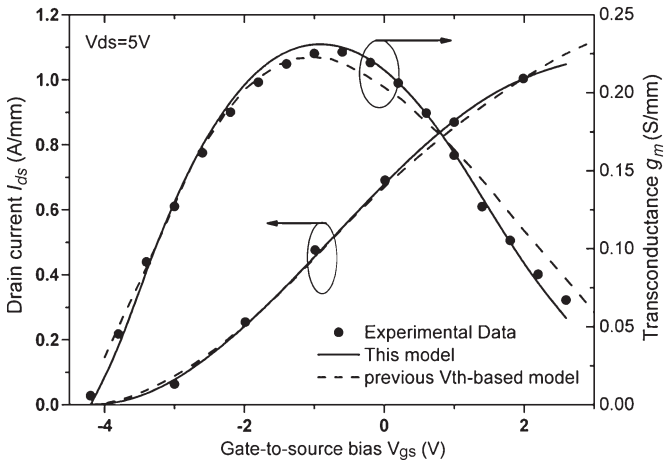

Fig. 9. Calculated and measured dc transfer characteristics for an $Al_{0.50}Ga_{0.50}N$/GaN MODFET. V_{gs} is swept from -4 to 3 V, and V_{ds} is 5 V.

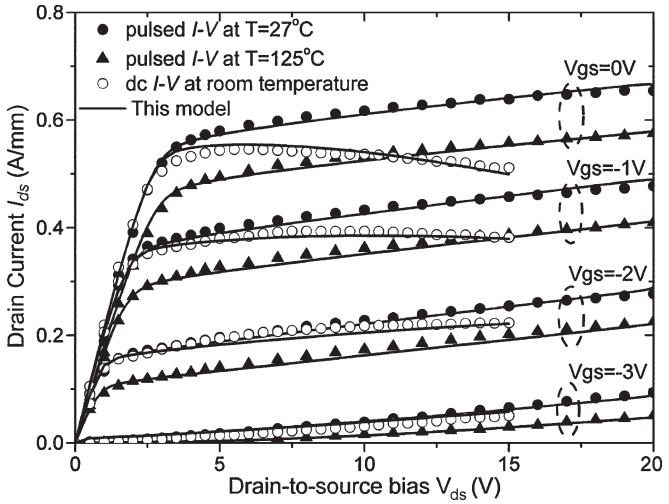

Fig. 10. Calculated and measured I–V characteristics for a 0.35-μm AlGaN/GaN MODFET. V_{gs} is swept from -3 to 0 V at a step of 1 V. (Solid line) The results of this model are compared with (dash line) our previous model and (symbol) the experimental data [20].

and 4 to a single point. Under all the gate-to-source biases from -3 to 2 V, this model also describes the I–V characteristics better in the saturation region because the new mobility model given by (28) is more physical. The dc transfer characteristics and the transconductance are shown in Fig. 9, and a better agreement is also observed. The continuity of the transconductance ensures the convergence of our model and helps to improve the model's reliability in circuit simulator. However, the model does not perform as well as we expect when the gate bias is very low. There are two reasons responsible for this problem. First, the triangular potential approximation used in (3) brings some error when the 2DEG density is extremely low. Second, the mobility given by (24) is a simple empirical model; more work on the physics of mobility is needed to improve this model.

In the end, the measured data under different temperatures from a short-channel (0.35 μm) AlGaN/GaN MODFET [20] are compared to verify the DIBL and self-heating effects in this model. For the calculation of the pulsed I–V characteristics at 27 °C and 125 °C, the device temperature is assumed to be kept at ambient temperature. These two comparison results along with the dc I–V output characteristics measured and calculated at room temperature are all shown in Fig. 10. Under different temperatures and measured conditions, this model agrees with the measured results well, which approves the method for self-heating calculation. Clear DIBL effect can also be observed in Fig. 10 from the measured results at $V_{gs} = -3$ V, and the DIBL extracted from our model is about 33 mV/V. The accuracy of the model showed here implies that the present assumption is acceptable to model DIBL and self-heating effects for AlGaN/GaN MODFETS.

IV. Conclusion

An analytical approximation for the SP has been developed over a wide range of device parameters and temperatures with a high degree of accuracy. Using this result, an SP-based model that is symmetric with respect to source–drain interchange and has no d^2I_{ds}/dV_{ds}^2 singularity is obtained. The mobility model for AlGaN/GaN MODFETs is rewritten, and more physics SP contents are incorporated. Velocity saturation, channel length modulation, DIBL, and self-heating effects are all included in this model. This model has been verified by three AlGaN/GaN MODFETs with different gate lengths from 1 μm down to 0.35 μm. The calculated dc characteristics and transconductance for all devices are in excellent agreement with the experimental data over the full range of applied gate and drain biases and under different temperatures. It is obviously shown that the present SP-based model provides a more accurate description than the previous $V_{\rm th}$-based model because the SP-based model well describes the E_F variation along the channel, which the $V_{\rm th}$-based model ignores. As this SP-based approach is more accurate and symmetric and also has a simpler structure than the $V_{\rm th}$-based approach, it is concluded that this SP-based approach is a strong candidate for compact modeling the AlGaN/GaN MODFETs.

References

[1] W. Liu, *MOSFET Models for SPICE Simulation Including BSIM3v3 and BSIM4*. New York: Wiley, 2001.

[2] D. Foty, *MOSFET Modeling With SPICE: Principles and Practice*. Upper Saddle River, NJ: Prentice-Hall, 1997.

[3] R. Rashmi, A. Kranti, S. Haldar, and R. S. Gupta, "An accurate charge control model for spontaneous and piezoelectric polarization dependent two-dimensional electron gas sheet charge density of lattice-mismatched AlGaN/GaN HEMTs," *Solid State Electron.*, vol. 46, no. 5, pp. 621–630, May 2002.

[4] X. Cheng, M. Li, and Y. Wang, "Physics-based compact model for AlGaN/GaN MODFETs with close-formed I–V and C–V characteristics," *IEEE Trans. Electron Devices*, vol. 56, no. 12, pp. 2881–2887, Dec. 2009.

[5] G. Gildenblat, H. Wang, T.-L. Chen, X. Gu, and X. Cai, "SP: An advanced surface-potential-based compact MOSFET model," *IEEE J. Solid-State Circuits*, vol. 39, no. 9, pp. 1394–1406, Sep. 2004.

[6] P. Bendix, "Detailed comparison of the SP2010, EKV and BSIM3 models," in *Tech. Proc. 5th Int.Conf. Model. Simul. Microsyst.*, 2002, p. 649.

[7] B. L. Anderson and R. L. Anderson, *Fundamentals of Semiconductor Devices*. New York: McGraw-Hill, 2005, ch. 7.

[8] M. Li and Y. Wang, "2-D analytical model for current-voltage characteristics and transconductance of AlGaN/GaN MODFETs," *IEEE Trans. Electron Devices*, vol. 55, no. 1, pp. 261–267, Jan. 2008.

[9] P. Bendix, P. Rakers, P. Wagh, L. Lemaitre, W. Grabinski, C. C. McAndrew, X. Gu, and G. Gildenblat, "RF distortion analysis with compact MOSFET models," in *Proc. IEEE CICC*, 2004, pp. 9–12.

[10] T. L. Chen and G. Gildenblat, "Analytical approximation for the MOSFET surface potential," *Solid State Electron.*, vol. 45, no. 2, pp. 335–339, Feb. 2001.
[11] S. Kola, J. M. Golio, and G. N. Maracas, "An analytical expression for Fermi level versus sheet carrier concentration for HEMT modeling," *IEEE Electron Device Lett.*, vol. 9, no. 3, pp. 136–138, Mar. 1988.
[12] K. Lee, M. S. Shur, T. J. Drummond, and H. Morkoc, "Electron density of the two dimensional electron gas in modulation doped layers," *J. Appl. Phys.*, vol. 54, no. 4, pp. 2093–2096, Apr. 1983.
[13] O. Kate, A. Horn, G. Bahir, and J. Salzman, "Electron mobility in an AlGaN/GaN two-dimensional electron gas I—Carrier concentration dependent mobility," *IEEE Trans. Electron Devices*, vol. 50, no. 10, pp. 2002–2008, Oct. 2003.
[14] H. C. Pao and C. T. Sah, "Effects of diffusion current on characteristics of metal–oxide(insulator)–semiconductor transistors," *Solid State Electron.*, vol. 9, no. 10, pp. 927–937, Oct. 1966.
[15] K. Joardar, K. K. Gullapalli, C. C. McAndrew, M. E. Burnham, and A. Wild, "An improved MOSFET model for circuit simulation," *IEEE Trans. Electron Devices*, vol. 45, no. 1, pp. 134–148, Jan. 1998.
[16] X. Cheng, M. Li, and Y. Wang, "An analytical model for current–voltage characteristics of AlGaN/GaN HEMTs in presence of self-heating effect," *Solid State Electron.*, vol. 54, no. 1, pp. 42–47, Jan. 2010.
[17] V. K. De and J. D. Meindl, "An analytical threshold voltage and subthreshold current model for short-channel MESFETs," *IEEE J. Solid-State Circuits*, vol. 28, no. 2, pp. 169–172, Feb. 1993.
[18] Y.-F. Wu, S. Keller, P. Kozodoy, B. P. Keller, P. Parikh, D. Kapolnek, S. P. Denbaars, and U. K. Mishra, "Bias dependent microwave performance of AlGaN/GaN MODFETs up to 100 V," *IEEE Electron Device Lett.*, vol. 18, no. 6, pp. 290–292, Jun. 1997.
[19] Y.-F. Wu, B. P. Keller, P. Fini, S. Keller, T. J. Jenkins, L. T. Kehias, S. P. Denbaars, and U. K. Mishra, "High Al-content AlGaN/GaN MODFETs for ultrahigh performance," *IEEE Electron Device Lett.*, vol. 19, no. 2, pp. 50–53, Feb. 1998.
[20] J.-W. Lee and K. J. Webb, "A temperature-dependent nonlinear analytic model for AlGaN-GaN HEMTs on SiC," *IEEE Trans. Microw. Theory Tech.*, vol. 52, no. 1, pp. 2–9, Jan. 2004.

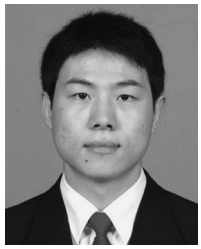

Xiaoxu Cheng received the B.S. degree in electronic engineering in 2007 from Tsinghua University, Beijing, China, where he is currently working toward the Ph.D. degree in the Institute of Microelectronics.

His current research topic is focused on the modeling of III-V compound semiconductor materials and devices.

Yan Wang received the B.S. and M.S. degrees in electrical engineering from Xi'an Jiaotong University, Xi'an, China, in 1988 and 1991, respectively, and the Ph.D. degree in semiconductor device and physics from the Chinese Academy of Science, Beijing, China, in 1995.

Since 1999, she has been a Professor with the Institute of Microelectronics, Tsinghua University, Beijing. Her research centers on device modeling.